Stability of sodalite relative to nepheline in NaCl-H_2O brines at 750° C: implications for the hydrothermal formation of sodalite

Jonathan B. Schneider

David M. Jenkins

Dept. Geological Sciences and Environmental Studies

Binghamton University

Binghamton, NY 13902-6000

USA

Abstract

Formation of the feldspathoid mineral sodalite ($Na_6Al_6Si_6O_{24}\cdot 2NaCl$) by reaction of nepheline ($NaAlSiO_4$) with NaCl-bearing brines was investigated at 3 and 6 kbar and at a constant pressure (P) of 750°C to determine the brine concentration at which sodalite forms with variation in pressure. The reaction boundary was located by reaction-reversal experiments using minerals formed in the system $NaAlSiO_4$ – NaCl at a brine concentration of 0.09 X_{NaCl} (= molar ratio $NaCl/(NaCl + H_2O)$) at 3 kbar and at a brine concentration of 0.29 X_{NaCl} at 6 kbar of pressure. Characterization of the sodalite using both X-ray diffraction and infrared spectroscopy after treatment in these brines indicated no obvious evidence of water or hydroxyl incorporation into the cage structure of sodalite. The data from this study were combined with earlier results at lower (1-1.5 kbar) and higher (7-8 kbar) pressures on sodalite formation from nepheline and NaCl which models as a curve in $X_{NaCl} – P$ space, or as essentially a straight line in wt%NaCl – P space. In general, sodalite buffers the concentration of neutral aqueous NaCl° in the brine to

relatively low values at $P < 4$ kbar, but rises rapidly at higher pressures. Thermochemical analysis of these data was done to determine the activity of the aqueous NaCl° relative to a 1 molal (*m*) standard state, demonstrating very low activities (< 0.2 *m*, or 1.2 wt%) of NaCl° at 3 kbar and lower, but rising to relatively high activities (> 20 m, or 54 wt%) NaCl° at 6 kbar or higher. The results from this study place constraints on the concentration of NaCl° in brines coexisting with nepheline and sodalite, and, because of the relative insensitivity of this reaction to pressure, can provide a convenient geobarometer for those localities where the fluid compositions that formed nepheline and sodalite can be determined independently.

keywords: sodalite, nepheline, NaCl brine, feldspathoids, synthesis, NaCl activity

Introduction

Minerals in the feldspathoid group are rare rock-forming tectosilicates that occur in silica (SiO_2) deficient igneous and metamorphic environments. The lack of silica in the environment in which feldspathoids occur defines their distinction from feldspars. Sodalite ($Na_8Al_6Si_6O_{24}Cl_2$) and nepheline ($NaAlSiO_4$) are two of the more common minerals in the feldspathoid group of minerals that often occur together as sodalite-nepheline syenites or in silica undersaturated metasomatically-altered igneous rocks (Deer et al., 1963, p. 289; Eby et al., 1998; Chakrabarty et al., 2016). There are also occurrences of sodalite in alkali layered intrusions (Bailey et al., 2006; Moller and Williams-Jones, 2016), metamorphosed calc-silicate or silica-undersaturated rocks (Jamtveit et al., 1997; Goswami and Basu, 2013), and meteorites (e.g., Matsumoto et al., 2017).

Sodalite is an anomalous rock-forming mineral among silicates in that its distinct constituent is water-soluble salt, NaCl. The breakdown products of sodalite are nepheline ($NaAlSiO_4$) and halite (NaCl):

$$Na_8Al_6Si_6O_{24}Cl_2 \rightleftharpoons 6\ NaAlSiO_4 + 2\ NaCl \quad (1)$$

sodalite nepheline halite

Sodalite exhibits the capacity to buffer the activity of NaCl as it decomposes (Wellman, 1970; Sharp et al., 1989). This ability to buffer the activity of NaCl allows the measurement of fluid inclusions of a host mineral to be used to indicate the minimum fluid salinity at the time of formation (Roedder, 1984, p. 233ff; Sharp et al., 1989). With this information, experiments demonstrating the phase equilibria between sodalite and nepheline + halite in pressure-temperature-mole fraction NaCl (X_{NaCl}) space in the metasomatic system $NaAlSiO_4$-NaCl-H_2O can proffer minimum pressures, temperatures, or salinities of formation when both sodalite and nepheline are found together.

Wellman (1970) demonstrated the stability of sodalite relative to nepheline + halite in temperature versus X_{NaCl} space, in the system $NaAlSiO_4$-NaCl-H_2O at temperatures of 500 to 700 °C and pressures of 0.6 – 2.0 kbar in dilute aqueous solutions. At 600°C, Wellman (1970) found sodalite formed at a very low X_{NaCl} value of 0.00035 (=0.0002 wt% NaCl) at 0.6 kbar which increased to 0.019 (= 0.11 wt% NaCl) at 2.0 kbar. Sharp et al. (1989) determined the upper-pressure stability of sodalite in the system $NaAlSiO_4$-NaCl in the range of 650 – 900°C at pressures of 7- 10 kbar under water-free conditions. They found that sodalite is stable along the low-pressure side of a univariant boundary that is almost completely pressure dependent, with a

small positive temperature dependence of about 0.005 kbar/K over the range of 700-900°C. Such a flat dP/dT slope suggests that the assemblage nepheline + sodalite can make the basis of an excellent geobarometer, so long as the variation in sodalite stability with X_{NaCl} can be determined. This concept is illustrated in Figure 1, which is a schematic illustration of how the stability of nepheline is expanded as the activity of NaCl in the brine decreases.

In this study the stability of sodalite relative to nepheline in NaCl-H_2O brines is demonstrated at pressures of 3.0 and 6.0 kilobars at a constant temperature of 750 °C, i.e., along the vertical dash-dot line of Figure 1. Because the thermochemical data for sodalite and nepheline are fairly well known, one can also use the experimental data of this study, combined with those of Wellman (1970) and Sharp et al. (1989), to derive activities of the associated aqueous species NaCl° in the brine at the elevated pressure, temperature, and brine concentrations of this study.

Methods

Starting materials

All phases were produced from stoichiometric mixtures of reagent-grade Na_2CO_3, Al_2O_3, SiO_2, and sodium chloride. The SiO_2 was made by desiccating silicic acid by heating it to 1100°C in air for 24 hours generating cristobalite. The source of Na for both the nepheline and the silicate-cage structure of sodalite was Na_2CO_3, which was mixed with SiO_2 and Al_2O_3 and then decarbonated by heating the mixture in air at 900°C for 15 min. Reagent NaCl typically has fluid trapped in it during its processing; these fluid inclusions were decrepitated by roasting at 500°C in air for several hours. For hydrothermal experiments appropriate amounts of deionized water was added to the mixture to achieve a desired X_{NaCl} (= moles of NaCl/(moles of NaCl + moles of

H_2O)) brine concentration. Starting bulk compositions investigated in this research are present in Table 1.

Apparatus

A piston-cylinder press with 0.5 inch diameter was employed for the synthesis of nepheline at 12.8 kilobars and for the reversal experiments at ~6.0 kbar of pressure. The apparatus uses NaCl as the pressure medium both inside and outside of a straight cylindrical graphite furnace. Chromel-alumel thermocouples were placed in the NaCl pressure media right above the sample to measure the temperatures. The temperature uncertainty for smaller (1.5 mm OD) capsules is estimated as ± 5°C, while larger capsules (4 mm OD) is estimated as ± 15°C. Although the pressure media uses a maximum amount of NaCl, the low-pressure range of the experiments done in the 0.5-inch diameter pressure plate is of some concern, particularly when the original pressure calibration was done using the albite = jadeite + quartz reaction boundary at 600°C and 16.2 kbar (Quirion and Jenkins, 19xx). Therefore, a series of calibration experiments was done 750°C and in the range of 7.5 – 9.5 kbar at using the pressure-sensitive conversion of $Mg_3(PO_4)_2$ (farringtonite) to its high-pressure polymorph ($Mg_3(PO_4)_2$-II) (Brunet and Vielzeuf, 1996). Synthetic (reagent) farringtonite and its high-pressure form $Mg_3(PO_4)_2$-II were prepared separately by heating magnesium-phosphate hydrate ($Mg_3(PO_4)_2 \cdot xH_2O$) at 1 atm and 1000°C for 18 hours and at 750°C and 10 kbar for 48 hours, respectively. Mixtures consisting of both of these phases were then treated in reaction-reversal experiments. Growth of low-pressure farringtonite was observed at 7.5 kbar while growth of high-pressure $Mg_3(PO_4)_2$-II was observed at 8.2 kbar, all at 750°C. The average pressure (7.8 kbar) is shifted about 0.3 kbar higher than the 7.5 kbar boundary reported by Brunet and Vielzeuf (1996) at 750°C. In view of the inherent precision of about 0.30 kbar arising from the measurement precision and typical daily variation

in pressure of the piston-cylinder press, along with the stated uncertainty of ± 0.2 kbar in the location of the boundary reported by Brunet and Vielzeuf (1996), it is unclear whether there is any significant deviation between the nominal and observed pressure. Therefore, we have opted to report the nominal pressure (based on hydraulic geometry) as being the actual pressure but with uncertainties expanded to ± 0.5 kbar, which is essentially what one gets by a propagation-of-errors estimate. The average treatment for each run was approximately 96 hours after which the piston-cylinder press was quenched by turning off the furnace and the sample retrieved. Two small-diameter capsules could be run in the piston-cylinder press simultaneously to improve treatment efficiency.

For reversal experiments at 3.0 kilobars of pressure an internally-heated gas vessel with argon as the pressure medium was used. Bourbon-tube and manganin-cell gauges were used to measure pressure, with resultant uncertainties in pressure of about 0.05 kbar. The thermal gradient along the capsule was monitored by two Inconel®-sheathed chromel-alumel thermocouples that exhibited a gradient of approximately 10°C and uncertainties of temperature of ± 5°C. The average treatment for each run was approximately 96 hours.

A horizontally mounted cold-seal vessel apparatus constructed of René 41 with filler rods of the same material was used to synthesize sodalite. The pressure medium is water and is monitored by bourbon-tube gauges accurate to ± 0.05 kilobars. The temperature of the cold-seal apparatus is measured with external chromel-alumel thermocouples with associated temperature uncertainties at the sample of ± 5°C. After treatment the cold-seal vessel was quench to room temperature using first compressed air and then water..

Analytical methods

A Panalytical Xpert PW3040-MPD diffractometer was used for powder X-ray diffraction (XRD) analysis. The operating conditions were 20 mA and 40 kV with CuKα radiation and used a diffracted-beam graphite monochromator. Samples are placed on a zero-background single crystal quartz plate for XRD analysis. Panalytical software HighScore® was used to identify peaks of distinct minerals and their peak-area. Reaction direction of the reversal mixtures of sodalite, nepheline, and halite was established by comparing the peak-area ratios for the starting material to the experimental treatment products using the following reflections: sodalite [(211), 24.56° 2Θ]; nepheline [(202), 29.66° 2Θ]; and halite [(111), 31.73° 2Θ]. Unit-cell dimensions of sodalite were determined by Rietveld refinements for selected samples using the program GSAS-II (Toby and Von Dreele, 2013) and using NaCl (a_0 = 5.6401Å) as an internal standard.

Results

Starting Mixture Synthesis

To perform these experiments a reversal mixture was made from both synthetic nepheline and sodalite and reagent-grade sodium chloride. The nepheline was made with reagent grade Na_2O, SiO_2, and Al_2O_3 measured out stoichiometrically and thoroughly mixed in an agate mortar with acetone. The mixture was sealed (arc welded) in a platinum flame-annealed (1200°C) capsule with 2 weight % deionized H_2O added to aid the kinetics of the reaction. The capsule was treated in the piston-cylinder apparatus at 750°C and 12.8 kb for 72 hours.

The sodalite was made with reagent-grade Na_2O, SiO_2, Al_2O_3, and NaCl measured out stoichiometrically and thoroughly mixed in an agate mortar with acetone. The mixture was sealed dry in a platinum capsule and treated in a cold-seal apparatus at 800 °C and 2 kb for 96 hours.

Characterization of synthetic sodalite

Because sodalite can incorporate water as hydroxyls and/or zeolitic water in the Si-Al-tetrahedral cage, it is of interest to determine whether the sodalite treated in the brines used in this study incorporated hydroxyls or water. Two methods were used to address this question. The first involved determination of the unit-cell dimension (a_0) which has been correlated with the water/OH content (e.g., Felsche and Luger, 1987; Moloy et al., 2006). Table 2 lists the unit-cell dimensions determined for sodalite as synthesized anhydrously (SOD 1-1) and for selected samples of the same sodalite treated at the conditions listed in Table 1. Figure 2 shows the cell dimensions for hydrothermally-treated sodalite from this study (circles) plotted as a function of the pressure of treatment. For comparison, the double-headed arrow in Figure 2 shows the range of cell dimensions for non-basic hydrosodalite ranging in composition from fully hydrated ($Na_6[AlSiO_4]_6 \cdot 8H_2O$ = 6:0:8) to dehydrated ($Na_6[AlSiO_4]_6$ = 6:0:0) based on the data from Felsche and Luger (1987) and Engelhardt et al. (1992). The grey band in Figure 2 also shows the typical cell dimension range for synthetic sodalite reported in the literature (Henderson and Taylor, 1978; Weller and Wong, 1989; Nielsen et al., 1991). The cell dimensions from this study are indistinguishable from synthetic sodalite, suggesting there is no obvious variation with pressure or brine composition.

Second, infrared spectra in the mid-infrared range were obtained for several of the sodalites formed on the sodalite-growth side of reaction (1). At the top of Figure 3 are the FTIR spectra for two natural sodalites shown for reference. The top spectrum is from the RRUFF database (sample R040141, Princess Sodalite mine, Bancroft, Ontario, Canada; Lafuente et al., 2015), while the second spectrum is for a natural sodalite (locality unknown) from the Binghamton University mineral collection. The lower three spectra are for synthetic sodalites from this study; SOD 1-1 is the sodalite used in the reversal mixtures made anhydrously at 800 °C and 2 kb for

96 h, while SOPH 2-9 and SOPH 3-14 are sodalites formed inside the sodalite stability field at 750 °C and at the brine concentrations and pressures indicated in the figure. The starting material sodalite (SOD 1-1) had an additional band at 1450 cm^{-1} which correlates with the strongest band of carbonates (e.g., Jenkins et al., 2017) and is therefore assigned to a minor amount of residual Na_2CO_3 still present in the starting material used to make the sodalite. This band does not appear in any of the hydrothermally-treated samples indicating that whatever carbonate might be present is driven out into the ambient fluid during hydothermal treatment. Sample SOPH 2-9 appears to have a broad band in the range of 3000-3700 cm^{-1} indicative of cage or zeolitic water, or it may simply be absorbed water, as seen in non-basic hydrosodalite (e.g., Engelhardt et al., 1992). The presence of this band is supported by the broadened lattice vibrations in the range of 400-1100 cm^{-1} for hydrosodalite reported by Buhl et al. (2017). Two features are of particular note. One is that a broad water absorption band at 3000-3700 cm^{-1} is not present in the spectrum of SOPH 3-14 despite being treated in a slightly more water rich brine. Perhaps the water was never incorporated into this sample at the lower pressure (3 kb) of treatment compared to SOPH 2-9 (6 kb), or any water that was incorporated was readily released upon decompression. The other is that the distinctive narrow band at 3640 cm^{-1} that is attributed to O-H stretching in basic hydrosodalite or hydroxo-sodalite (Felsche and Luger, 1987) is not observed in these spectra, indicating that the water is either zeolitic or simply absorbed rather than strongly bonded with Na or other portions of the silicate structure.

Taking both the FTIR and unit-cell dimension data together, there does not appear to be any systematic incorporation of H_2O in the sodalites formed in this study. Even though the unit-cell dimensions of the sodalites of this study overlap those of the nearly fully hydrated non-basic hydrosodalite in Figure 2, the low intensity and/or absence of the broad H_2O IR band argues

against this unit-cell dimension arising from H_2O but instead coming from the NaCl-bearing sodalite. The weight of evidence, including the relatively high temperature (750°C) used for making and treating the sodalite used in this study, suggests that there is minimal incorporation of either OH or H_2O into the sodalite structure and that we will, to a first approximation, consider the sodalite to be essentially water free.

Stability field of sodalite

The stability field of sodalite relative to halite + nepheline is shown in Figure 4 as a function of the mole fraction of NaCl in the brine (X_{NaCl}), which is only an apparent value above halite saturation. Experimental results from this study producing sodalite growth at 3 and 6 kb are shown by open circles, nepheline growth by solid circles, and no clear reaction by half-shaded circles. Shown for comparison are selected experiments along the same reaction boundary extrapolated from the results of Wellman (1970, diamonds) as well as the halite saturation boundary (dashed curve) extrapolated to 8 kb, which is slightly beyond the 5 kb limit of the equations given by Driesner and Heinrich (2007). The reaction boundary at 750 °C involving pure NaCl determined by Sharp et al. (1989) is shown by the solid square. It is assumed that the location of this boundary remains constant in pressure over the range of saturation in halite, indicated by the horizontal solid line. This assumption may not be strictly correct if, for example, there is eutectic melting occurring between sodalite and halite in the presence of water and there is a loss of halite (the limiting solid). This process was suggested by Almeida and Jenkins (2017) to explain the destabilization of marialite, the NaCl end-member of scapolite, above halite saturation; however, such an effect, if it exists, is less than ~2 kb based on the strong sodalite growth observed in this study at high apparent brine concentrations at 6.0 ± 0.5 kb. The sodalite stability boundary below halite saturation (solid curve) is simply an empirical fit of the

bracketing data from this study, the 1.0 and 1.5 kb boundary points of Wellman (1970) extrapolated to 750 °C, and the 7.7 kb boundary point of Sharp et al. (1989), all fitted to a three-term exponential-rise equation:

$$P = 12.66(1 - e^{-1.313 \cdot X_{NaCl}}) + 1.026 \quad (2)$$

This equation has no physical significance but is provided as a way to quantify the rapid rise in sodalite stability with increasing pressure. A simpler fit to the same data can be made if the sodalite stability curve below halite saturation is represented as the weight% of NaCl rather than mole fraction, as shown in Figure 5. In this case the curve is closely modeled by the linear equation given in the figure. Equation (2) was used in the subsequent thermodynamic analysis, but the linear equation in Figure 5 is provided for those who prefer to work with brine concentrations in weight%.

Discussion

Activity of NaCl° in concentrated brines

Because of the relative simplicity of the chemical system investigated here ($NaAlSiO_4$-NaCl), one can use the experimental results presented here to determine activity coefficients for the neutral aqueous species NaCl° in concentrated brines. Such information would complement the existing studies in the literature regarding the activity of H_2O in concentrated brines (e.g., Aranovich and Newton, 1996; Manning and Aranovich, 2014). The approach taken here is to use the conventional standard state for aqueous solutions (i.e., unit activity for a 1 molal solution) and relate the shift in the pressure of reaction (1) (Fig. 1) to the reduction in the activity of NaCl° in the brine.

Sodalite breaking down to nepheline below halite saturation in Figure 4 can be described by the following reaction involving aqueous NaCl°:

$Na_8Al_6Si_6O_{24}Cl_2 = 6\ NaAlSiO_4 + 2\ NaCl°$ (3)

sodalite nepheline brine

For the case of pure sodalite and nepheline at unit activity, the equilibrium constant (K_3) for reaction (3) is:

$$K_3 = \left(a_{NaCl°}^{brine}\right)^2 \quad (4)$$

where $a_{NaCl°}^{brine}$ is the activity of NaCl° in the brine relative to the 1 molal standard state. In the absence of detailed knowledge of all possible aqueous species in these experiments, it will be assumed that the silicates experience negligible dissolution and that the brine is closely modeled by the system H_2O-NaCl. This assumption is supported by the study of Makhluf et al. (2016) who demonstrated a marked decrease in albite solubility at 10 kbar and 690°C with increasing NaCl content. It is suggested here that this "salting out" effect combined with the common-ion effect (Na^+) will tend to minimize the solubilities of these Na-bearing minerals. It is also assumed that the dominant species in the brine are NaCl°, Na^+, and Cl^-, as supported by the calculations of Manning (1998) for brines equilibrated with a model glaucophane (Na-rich silicate) eclogite in the system Na_2O-MgO-Al_2O_3-SiO_2-H_2O-HCl at 550°C and 17.5 kbar. The extent of NaCl° dissociation is controlled by the reaction:

$NaCl° = Na^+ + Cl^-$ (5)

where the equilibrium constant for reaction (5) is:

$$K_5 = \frac{a_{Na^+} a_{Cl^-}}{a_{NaCl°}} \quad (6)$$

The extent of dissociation has been calculated by Evans and Powell (2006) to be quite low in the range of 600-660 °C and 2-7 kbar, indicating that aqueous NaCl° will likely be the dominant species in these experiments (Evans and Powell, 2006).

At equilibrium, the equilibrium constant (K_a) is related to the change in the Gibbs free energy of the reaction for all phases in their standard state at a given pressure and temperature ($\Delta G^o_{P,T}$) by the equation:

$$K_a = e^{-\Delta G^o_{P,T}/RT} \quad (7)$$

where R is the universal gas constant and T is the temperature in Kelvins. In this study values of $\Delta G^o_{P,T}$ were calculated using the thermodynamic data and methods of Holland and Powell (1998, 2011). One minor adjustment was made to the enthalpy of formation (ΔH^o_f) of sodalite, which was reduced by 2.11 kJ (i.e., ΔH^o_f = -13,407.52 kJ), to bring the pressure of reaction (1) to 7.72 kb at 750°C, which was used as an anchor point in this study. This adjustment is well within the stated one standard deviation of 10.54 kJ given for sodalite (Holland and Powell, 2011). For convenience, the thermodynamic data for all solid phases and aqueous species used in this study are summarized in Table 3. The Gibbs free energies of the aqueous species depend on the density of water at P and T, which was calculated from the CORK equation of state for H_2O from Holland and Powell (1991). Using the restriction of mass balance in the brine, where the total molality of NaCl in the brine (m_{NaCl}) is the sum of NaCl° and Na^+ (or Cl^-), and that activity is equal to molality, then a correction can be made for the extent of dissociation of NaCl° by solving for the concentration of Na^+ (= $m_{Na^+} = m_{Cl^-}$) that satisfies the relation:

$$m_{\mathrm{NaCl}} = \frac{\left(m_{Na^+}\right)^2}{K_5} + m_{Na^+} \quad (8)$$

for a given total molality of NaCl in the brine (m_{NaCl}).

Using the location of the sodalite stability curve described by equation (2) along with the thermodynamic data in Table 3, one can derive the activities and activity coefficients ($\gamma = a/m$) for NaCl° with and without accounting for dissociation. These values are listed in Table 4 and shown in Figures 6a and 6b as a function of pressure. Also shown in Figure 6c are the calculated molalities of NaCl°, Na^+, and Cl^- from the dissociation of the total NaCl in the brine at 750°C and the pressure indicated. What Figures 6a and 6b indicate is that the thermodynamic drive of reaction (3) runs so strongly toward sodalite formation that only very low activities of NaCl° are needed to stabilize sodalite at low pressures, resulting in very low molality activity coefficients with $\gamma << 1.0$. This is supported by the earlier study of Wellman (1970) who was able to form sodalite at, for example, only 0.00045 mole fraction of NaCl (= 0.025 m_{NaCl}) at 557°C and 0.604 kbar. Such remarkably low concentrations of NaCl make the presence of sodalite in nature a very sensitive indicator of aqueous chloride solutions.

Applications to nepheline-sodalite-bearing assemblages

Owing to the very limited dependence of reaction (1) to temperature (Fig. 1), the shift in the location of reaction (1) by reducing the activity of NaCl° in the solution offers a very sensitive geobarometer if the concentration (activity) of NaCl° in the fluid coexisting with nepheline and sodalite is known. Conversely, the concentration of NaCl° in a brine can be determined from reaction (3) (Figs. 4 and 5) if the depth (pressure) of formation for a sodalite-nepheline-bearing assemblage is known. We will consider two examples.

The nepheline gneisses from the York River area of Bancroft, Ontario, Canada, have been the subject of several studies because of their apparent formation from by the metasomatism of either metasedimentary or meta-volcanic protoliths. Anderson and Cermignani (1991) reported

the occurrence of several primary fluid inclusions in nepheline and diopside which contained halite daughter crystals, suggesting the presence of fairly concentrated brines (> 6.2 *m* NaCl, or 26.5 wt% NaCl) at some point in the formation of the nepheline gneisses. However, thermodynamic modeling done at the estimated formation conditions of 2 kbar and 600°C using thermochemical data available at the time of their article suggested that brine concentrations were only 0.3-1 *m* NaCl (1.7 – 5.5 wt% NaCl) to avoid wollastonite formation, a mineral that is not observed in the York River nepheline gneisses. Based on the present study, the maximum NaCl° concentration the brine could have without converting pure nepheline to sodalite at 2 kbar is about 0.03 X_{NaCl} (= 1.7 *m* NaCl = 9 wt% NaCl, Fig. 4). If one allows for the reduction in the activity of $NaAlSiO_4$ in the kalsilite-bearing nephelines found in the York River gneisses, similar to nepheline observed in many other localities (Chakrabarty et al., 2016), and assuming that activity is equal to the mole fraction, then one would expect even higher brine concentrations. Figure 7 shows the calculated shift in reaction (3) with reduction in the activity of $NaAlSiO_4$ from 1.0 to 0.75. This results in a shift, at 2 kbar, to a brine concentration as high as 0.08 X_{NaCl} (= 4.8 *m* = 22 wt% NaCl). Andersen and Cermignani (1991) noted at the end of their study that the thermobarometry that was done by Anovitz and Essene (1990) on the Bancroft metamorphic domain (Easton, 2000) indicated metamorphic conditions that were in the range of 550-625° and 5.5-6.5 kbar. In this pressure range, the brine concentrations would range between X_{NaCl} of 0.23 (= 49 wt% NaCl) to 0.45 (= 73 wt% NaCl) for activities of $NaAlSiO_4$ in nepheline of 1.0 and 0.75, respectively. The latter concentration is near halite saturation at the peak metamorphic conditions of the Bancroft domain and may account for the occurrence of the rare primary fluid inclusions in nepheline with halite daughter crystals described by Anderson and Cermignani (1991).

Drüppel et al. (2005) reported the occurrence 16esoproterozoic syenite, nepheline syenite, and ferrocarbonatite dikes which intruded the anorthosites of the Kunene intrusive complex, northwestern Namibia. The ferrocarbonatite dikes are younger than either the anorthosites or the syenites and are host to a large amounts of sodalite. Sodalite formed by Na-rich fluids originating from the ferro-carbonatite magma and metasomatically altering the neighboring anorthosite, syenite, and nepheline syenite and transforming Ca-rich plagioclase, K-feldspar, and nepheline into albite or sodalite. Drüppel et al. (2005) and Drüppel and Wirth (2018) estimated through a combination of phase equilibria and fluid inclusion analysis that sodalite formed at 4 kbar and 700 ± 70°C. Little information was reported on the composition of the fluid, other than to note that it was a Na-rich and Si-poor fluid. Sodalite at this locality is essentially pure sodalite, so that a source of NaCl would be needed for its formation. Assuming the NaCl is from the fenetizing fluid, the present study indicates a minimum X_{NaCl} content of 0.13 (33 wt% NaCl) would be needed to convert pure nepheline to sodalite, or a salinity closer to $X_{NaCl} = 0.27$ (54 wt% NaCl) for the kalsilite-bearing nepheline in NW Namibia.

Conclusions

The nearly isobaric nature of the reaction controlling the formation of sodalite from nepheline and halite (Sharp et al., 1989) provides the framework for investigating the shift in this boundary with reduction in the activity of NaCl in aqueous solutions that can be applied to nepheline/sodalite assemblages without having accurate knowledge of temperature. In this study we present experimental data at 3 and 6 kbar at 750°C which demonstrate the growth and breakdown of sodalite in the presence of nepheline and a NaCl-bearing brine. The strong dependence of this reaction boundary (reaction 3) on brine concentration in pressure-composition space makes the coexistence of nepheline and sodalite a sensitive indicator of the

concentration of NaCl° in a coexisting brine. In general, sodalite is stabilized at relatively low NaCl° concentrations at low pressures (< 4 kbar). Conversely, the coexistence of nepheline and sodalite will buffer the activity of NaCl° in a coexisting aqueous solution to relatively low values at low pressures. In view of the limited data on the thermochemical activities of aqueous species at high pressures and temperatures, activities of the neutral aqueous NaCl° species relative to a 1-molal standard state were calculated to complement similar data derived for activites of NaCl relative to liquid NaCl in NaCl-H_2O mixtues (Aranovich and Newton, 1996). Application of the nepheline-sodalite-NaCl° boundary determined here to the York River nepheline gneisses occurring in the Bancroft metamorphic domain, Bancroft, Ontario, indicates that fluids could have as high as 46 to an estimated 73 wt% NaCl at 6 kbar and 750°C for pure nepheline or nepheline with 25 mol% kalsilite component, respectively. Likewise, formation of sodalite by metasomatism of nepheline in the nepheline syenites by from fluids exsolved by the ferrocarbonatite dikes in the Kunene intrusive comples, NW Namibia, at 4 kbar and 700°C would require brines ranging from 33 to 54 wt% NaCl depending on whether the nepheline is pure or has the typical 25 mol% kalsilite component. The results from this study would also provide a convenient geobarometry for those localities where the fluid compositions that were present at the time of coexisting nepheline and sodalite could be determined from, for example, the analysis of primary fluid inclusions hosted by the silicates,

Acknowledgements

We wish to thank V. Van Nostrand for help with the FTIR analyses. This research was supported by funding from National Science Foundation grant EAR-1725053 to DMJ.

References Cited

Almeida, K. M. F., and Jenkins, D. M. (2017) Stability field of the Cl-rich scapolite marialite. American Mineralogist, 102, 2484-2493.

Anovitz, L. M. and Essene, E. J. (1990) Thermobarometry and pressure-temperature paths in the Grenville Province of Ontario. Journal of Petrology, 31, 197-241.

Aranovich, L. Y. and Newton, R. C. (1996) H_20 activity in concentrated NaC1 solutions at high pressures and temperatures measured by the brucite-periclase equilibrium. Contributions to Mineralogy and Petrology, 125, 200-212.

Bailey, J.C., Sørensen, H., Andersen, T., Kogarko, L.N., Rose-Hansen, J. (2006) On the origin of microrhythmic layering in arfvedsonite lujavrite from the Ilímaussaq alkaline complex, South Greenland. Lithos, 91, 301-318.

Buhl, J.-Ch. (2017) Crystallization of hydrosodalite $Na_6[AlSiO_4]_6(H_2O)_8$ and tetrahydroborate sodalite, $Na_8[AlSiO_4]_6(BH_4)_2$ inside the openings of wafer-thin steel mesh. Advances in Chemical Engineering and Science, 7, 277-290.

Brunet, F., and Vielzeuf, D. (1996) The farringtonite / $Mg3(PO_4)_2$-II transformation: A new curve for pressure calibration in piston-cylinder apparatus. European Journal of Mineralogy, 8, 349-354.

Chakrabarty, A., Mitchell, R. H., Ren, M., Saha, P. K., Pal, S., Pruseth, K. L., and Sen, A. K. (2016) Magmatic, hydrothermal and subsolidus evolution of the agpaitic nepheline syenites of the Sushina Hill Complex, India: implications for the metamorphism of peralkaline syenites. Mineralogical Magazine, 80, 1161-1193.

Deer, W. A., Howie, R. A., and Zussman, J. (1963) Rock-forming Minerals, Vol. 4, Framework Silicates. J. Wiley, New York, 435 pp.

Driesner, T. and Heinrich, C. A. (2007) The system H_2O–NaCl. Part I: Correlation formulae for phase relations in temperature–pressure–composition space from 0 to 1000 °C, 0 to 5000 bar, and 0 to 1 X_{NaCl}. Geochimica et Cosmochimica Acta, 71, 4880-4901.

Drüppel, K. and Wirth, R. (2018) Metasomatic replacement of albite in nature and experiments. Minerals, 8, 214; doi:10.3390/min8050214.

Drüppel, K., Hoefs, J., Okrusch, M. (2005) Fenetizing processes induced by ferrocarbonatite magmatism and Swartbooisdrif, NW Namibia. Journal of Petrology, 46, 377-406.

Easton, R. M. (2000) Metamorphism of the Canadian shield, Ontario, Canada, II. Proterozoic metamorphic history. Canadian Mineralogist, 38, 319-344.

Eby, G. N., Woolley, A. R., Din, V., and Platt, G. (1998) Geochemistry and petrogenesis of nepheline syenites: Kasungu–Chipala, Ilomba, and Ulindi nepheline syenite intrusions, North Nyasa alkaline province, Malawi. Journal of Petrology, 39, 1405-1424.

Engelhardt, G., Felsche, J., and Sieger, P. (1992) The hydrosodalite system $Na_{6+x}[SiAlO_4]_6(OH)_x \cdot nH_2O$: formation, phase composition, and de- and rehydration studied by ^{1}H, ^{23}Na, and ^{29}Si MAS-NMR spectroscopy in tandem with thermal analysis, X-ray diffraction, and IR spectroscopy. Journal of the American Chemical Society, 114, 1173-1182.

Evans, K., and Powell, R. (2006) A method for activity calculations in saline and mixed solvent solutions at elevated temperature and pressure: A framework for geological phase equilibria calculations. Geochimica et Cosmochimica Acta, 70, 5488-5506.

Felsche, J. and Luger, S. (1987) Phases and thermal decomposition characteristics of hydro-sodalites $Na_{6+x}[AlSiO_4]_6(OH)_x \cdot nH_2O$. Thermochimica Acta, 118, 35-55.

Goswami, B. and Basu, S. K. (2013) Metamorphism of Proterozoic agpaitic nepheline syenite gneiss from North Singhbhum Mobile Belt, eastern India. Mineralogy and Petrology, 107, 517-538.

Henderson, C. M. B., and Taylor, D. (1978) The thermal expansion of synthetic aluminosilicate-sodalites, $M_8(Al_6Si_6O_{24})X_2$. Physics and Chemistry of Minerals, 2, 337-347.

Holland, T. J. B. and Powell, R. (1991) A compensated-Redlich-Kwong (CORK) equation for volumes and fugacities of CO_2 and H_2O in the range 1 bar to 50 kbar and 100-1600 °C. Contributions to Mineralogy and Petrology, 109, 265-273.

Holland, T. J. B. and Powell, R. (2011) An improved and extended internally consistent thermodynamic dataset for phases of petrological interest, involving a new equation of state for solids. Journal of Metamorphic Geology, 29, 333-383.

Jamtveit, B., Dahlgren, S., and Austrheim, H. (1997) High-grade contact metamorphism of calcareous rocks from the Oslo Rift, Southern Norway. American Mineralogist, 82, 1241-1254.

Jenkins, D. M., Holmes, Z. F., Ishida, K., and Manuel, P. D. (2017) Autocorrelation analysis of the infrared spectra of synthetic and biogenic carbonates along the calcite–dolomite join. Physics and Chemistry of Minerals, 45, 563-574.

Lafuente, B., Downs, R. T., Yang, H., and Stone, N. (2015) The power of databases: The RRUFF project. In: Highlights in Mineralogical Crystallography, T. Armbruster and R. M. Danisi (Eds.), pp. 1-30, W. De Gruyter, Berlin, Germany.

Makhluf, A. R., Newton, R. C., and Manning, C. E. (2016) Hydrous albite magmas at lower crustal pressure: new results on liquidus H_2O content, solubility, and H_2O activity in the

system $NaAlSi_3O_8$–H_2O–NaCl at 1.0 GPa. Contributions to Mineralogy and Petrology, 171, article 75.

Manning, C. E. (1998) Fluid composition at the blueschist-eclogite transition in the model system Na_2O-MgO-Al_2O_3-SiO_2-H_2O-HCl. Schweizerische Mineralogische und Petrographische Mitteilungen, 78, 225-242.

Manning, C. E. and Aranovich, L. Y. (2014) Brines at high pressure and temperature: Thermodynamic, petrologicand geochemical effects. Precambrian Research, 253, 6-16.

Matsumoto, M., Tomeoka, K., and Seto, Y. (2017) Nepheline and sodalite in chondrules of the Ningqiang carbonaceous chondrite: Implications for a genetic relationship with those in the matrix. Geochimica et Cosmochimica Acta, 208, 220-233.

Moller, V., and William-Jones, A.E. (2016) Petrogenesis of the Nechalacho layered suite, Canada: magmatic evolution of a REE-Nb-rich nepheline syenite intrusion. Journal of Petrology, 57, 229-275.

Moloy, E.C., Liu, Q., Navrotsky, A. (2006) Formation and hydration enthalpies of the hydrosodalite family of materials. Microporous and Mesoporous Materials, 88, 283-292.

Nielsen, N. C., Bildsøe, Jakobsen, H. J., and Norby, P. (1991) ^{7}Li, ^{23}Na, and ^{27}Al quadrupolar interactions in some aluminosilicate sodalites from MAS n.m.r. spectra of satellite transitions. Zeolites, 11, 622-632.

Quirion, D.M. and Jenkins, D.M. (1998) Dehydration and partial melting of tremolitic amphibole coexisting with zoisite, quartz, anorthite, diopside, and water in the system H_2O-CaO-MgO-Al_2O_3-SiO_2. Contributions to Mineralogy and Petrology, 130, 379-389.

Roedder, E. (1984) Fluid inclusions. Reviews in Mineralogy, 12, 644 p.

Sharp, Z. D., Helffrich, G.R., Bohlen, S.R., Essene, E.J. (1989) The stability of sodalite in the system $NaAlSiO_4$-NaCl. Geochimica et Cosmochimica Acta, 53, 1943-1954.

Toby, B. H., and Von Dreele, R. B. (2013) GSAS-II: the genesis of a modern open-source all purpose crystallography software package. Journal of Applied Crystallography, 46, 544-549.

Weller, M. T., and Wong, G. (1989) Characterisation of novel sodalites by neutron diffraction and solid-state NMR. Solid State Ionics, 32-33, 430-435.

Wellman, T.R. (1970) The stability of sodalite in a synthetic syenite plus aqueous chloride fluid system. Journal of Petrology, 11, 49-71.

Table 1. Bulk composition, treatment conditions, and products of phase synthesis and reaction reversal expiments

Sample code	Bulk composition used	T (°C)	P (kbars)	t (h)	X_{NaCl}	Apparatus	Products and comments
Sodalite synthesis							
SOD1-1	$Na_8Al_6Si_6O_{24}Cl_2$	800	2	96	---	cold-seal	sod, cor, hal
Nepheline synthesis							
NEPH1-1	$NaAlSiO_4$	750	12.8	72	0.0	piston cylinder	neph, cor
Reaction reversal experiments							
SOPH1-1	mix 1	750	5.5	70	1.00	piston cylinder	sod growth
SOPH1-3	mix 1	750	5.8	70	0.81(11)	piston cylinder	sod growth
SOPH1-7	mix 1	750	6.02	72	0.69(8)	piston cylinder	sod growth
SOPH1-4	mix 1	750	5.8	70	0.42(3)	piston cylinder	sod growth
SOPH1-2	mix 1	750	5.5	70	0.38(2)	piston cylinder	sod growth
SOPH2-9	mix 2	750	6.0	72	0.32(2)	piston cylinder	neph growth
SOPH2-8	mix 2	750	6.02	72	0.22(1)	piston cylinder	neph growth
SOPH1-5	mix 3	750	5.7	72	0.100(4)	piston cylinder	neph growth
SOPH1-6	mix 3	750	5.7	72	0.050(2)	piston cylinder	neph growth
SOPH2-10	mix 2	750	3.1	69	0.42(2)	gas vessel	sod growth
SOPH3-14	mix 3	750	3	72	0.30(2)	gas vessel	sod growth
SOPH3-15	mix 3	750	3	72	0.23(2)	gas vessel	sod growth
SOPH2-13	mix 2	750	3.1	72	0.15(2)	gas vessel	no apparent reaction
SOPH2-12	mix 2	750	3.1	72	0.14(2)	gas vessel	no apparent reaction
SOPH2-11	mix 2	750	3.1	69	0.08(2)	gas vessel	neph growth

Note: Uncertainties (1 σ) in last digit for X_{NaCl} given in parentheses. Reversal mixtures (mix 1, 2, and 3) are separate mixtures all consisting of synthetic sodalite, nepheline, and halite.
Abbreviations: sod = sodalite; cor = corundum; hal = halite, neph = nepheline

Table 2. Unit-cell dimension (a_0) and volume (V) of selected samples of sodalite synthesized or hydrothermally treated in this study

Sample code	a_0 (Å)	V (Å^3)
SOD 1-1	8.8761(3)	699.3(1)
SOPH 2-9	8.8800(6)	700.2(1)
SOPH 1-4	8.8787(5)	699.9(1)
SOPH 1-7	8.8769(4)	699.5(1)
SOPH 3-15	8.8721(5)	698.4(1)
SOPH 3-14	8.8806(4)	700.4(1)
SOPH 2-10	8.8685(4)	697.5(1)

Table 3. Thermochemical data used in this study, based on Holland and Powell (2011, 1998). All values are at 1 bar and 298 K.

Molar values	Phase or aqueous species					
	Sodalite	Nepheline	NaCl (halite)	NaCl° (aqueous)	Na^+ (aqueous)	Cl^- (aqueous)
ΔH_f (kJ)	-13407.5*	-2094.54	-411.3	-399.88	-240.3	-167.08
$S°$ (kJ/K)	0.91	0.1244	0.0721	0.12609	0.0584	0.05673
V (kJ/kbar)	42.13	5.419	2.702	2.226	-0.111	1.779
a (kJ/K)	1.5327	0.2727	0.0452	-0.002	0.0306	-0.1414
b (kJ/K^2)	4.77 X10^{-5}	-1.24 X10^{-5}	1.79 X10^{-5}	1.91 X10^{-4}	1.91E-04	0
c (kJ·K)	-2972.8	0	0	0	0	0
d (kJ/K$^{0.5}$)	-12.427	-2.7631	0	0	0	0
α (K^{-1})	4.63X10^{-5}	4.63X10^{-5}	11.5X10^{-5}	0	0	0
κ (kbar)	465	465	238	0	0	0
κ’	4.16	4.16	5	0	0	0
κ’’(kbar^{-1})	-0.0089	-0.0089	-0.021	0	0	0
Tc (K)	----	467	----	----	----	----
S_{max} (kJ/K)	----	0.0100	----	----	----	----
V_{max} (kJ/kb)	----	0.0800	----	----	----	----

Note: For aqueous species, $C_P^* = a + bT$,

*Reduced by 2.11 kJ to fix the pressure of reaction (1) to 7.72 kb at 750°C

Table 4. Derived values of activity (a) and activity coefficient (γ) of NaCl° (aqueous) along the sodalite-stability curve via reaction (3) relative to a 1 molal solution standard state, without and with dissociation, all at 750 °C. Values with uncertainties are experimental points from this study, other values are derived from the curve fitted in Figure 4.

Pressure	mNaCl(total)	X_{NaCl}	$a_{NaCl°}(m)$	$\gamma_{NaCl°}(m)$ (no diss.)	$\gamma_{NaCl°}(m)$ (with diss.)
7.72	72.8	0.57	70.4	0.97	1.05
7.43	55.5	0.50	58.8	1.06	1.16
6.86	37.0	0.40	40.1	1.08	1.20
6.07	23.8	0.30	21.4	0.90	1.00
5.80	20.8	0.27	16.8	0.80	0.90
± 0.4	± 3.8	± 0.04	± 2.5	± 0.14	± 0.16
4.95	13.9	0.20	6.78	0.49	0.55
3.39	6.17	0.10	0.52	0.084	0.092
3.00	4.83	0.08	0.20	0.042	0.045
± 0.2	± 0.65	± 0.01	± 0.11	± 0.017	± 0.019
2.59	3.54	0.06	0.056	0.016	0.017
2.16	2.31	0.04	0.0088	0.0038	0.0040
1.69	1.13	0.02	0.00050	0.00045	0.00047

Figure Captions

Figure 1. Schematic illustration of the decrease in the stability of sodalite relative to nepheline and NaCl with decrease concentration (activity) of NaCl in the brine. Solid curve is the upper-pressure stability of sodalite based on the work of Sharp et al. (1989) for pure halite (X_{NaCl} = 1.0), dotted curves are estimated isopleths of constant X_{NaCl} in the brine, and the vertical dash-dot curve represents the isothermal section of this study.

Figure 2; Unit-cell dimension (ao) for synthetic sodalite formed in this study (starting sodalite,SOD 1-1, square) and for treated sodalite from selected samples (Table 2, circles). Uncertainties are the size of the symbol if not shown explicitly. Grey band is the range of cell dimensions for synthetic sodalite reported in the literature, while the double-headed arrow is the range of cell dimensions for non-basic hydrosodalite ranging in composition from fully hydrated (6:0:8) to dehydrated (6:0:0) based on the data from Felsche and Luger (1987) and Engelhardt et al. (1992).

Figure 3. The top two spectra are the mid-infrared FTIR spectra for natural sodalites provided for reference. The bottom three spectra are as follows: SOD 1-1 is the sodalite used in the starting materials, made by dry synthesis at 800 °C and 2 kb for 96 h, while SOPH 2-9 and SOPH 3-14 were treated at 750°C and at the brine concentrations and pressures indicated in the figure. A trace amount of carbonate (carb) was detected in SOD 1-1 but not in the other spectra.

Figure 4. Experimental determination of the reaction boundary for reaction (1) in the text at 750°C. Solid circles indicate growth of nepheline, open circles growth of sodalite, and half-shaded symbols indicate no clear reaction direction. Brine concentrations are calculated, not measured, mole fractions of NaCl. Upper-pressure stability of sodalite (square) is from Sharp et al. (1989), the lowest-pressure data (diamonds) are extrapolated to 750°C from the

data of Wellman (1970), and the halite saturation curve (dashed) is from the study of Driesner and Heinrich (2007, D&H 2007) with a short extrapolation beyond 5 kbar to 7.7 kbar. The experimental data are modeled with a three-term exponential rise equation (solid curve, see text) for convenience and has no theoretical basis.

Figure 5. Same diagram as for Figure 4 but shown as a function of the weight% of NaCl in the brine. Dashed line is polynomial fit to the limiting experimental data in Figure 4 yielding the equation given in the diagram and corresponding correlation coefficient (r).

Figure 6. (a) Activity of aqueous NaCl° ($a_{NaCl°}$) on a molal scale as a function of pressure derived from the sodalite stability curve of Figure 4. Data points are those at 3 and 5.8 kbar from this study. (b) Activity coefficient (γ) for NaCl° for the case where NaCl is dissociated (dashed) or not dissociated (solid). (c) Estimated molalities of NaCl° (solid curve) and Na^+ and Cl^- (dashed curve) with change in pressure. All diagrams are at 750°C.

Figure 7. Solid curve represents the same boundary for the reaction of 6 nepheline + 2 NaCl° = sodalite involving pure nepheline ($a_{Neph} = 1.0$) as shown in Figure 4. The dashed boundary illustrates a calculated shift in this boundary resulting from the reduction in the activity of nepheline from 1.0 to 0.75, assuming that nepheline forms an ideal solution with kalsilite typically present at 25 mol%. Both curves are at a constant temperature of 750°C. The halite saturation curve is from the study of Driesner and Heinrich (2007, D&H 2007).

Figure 1

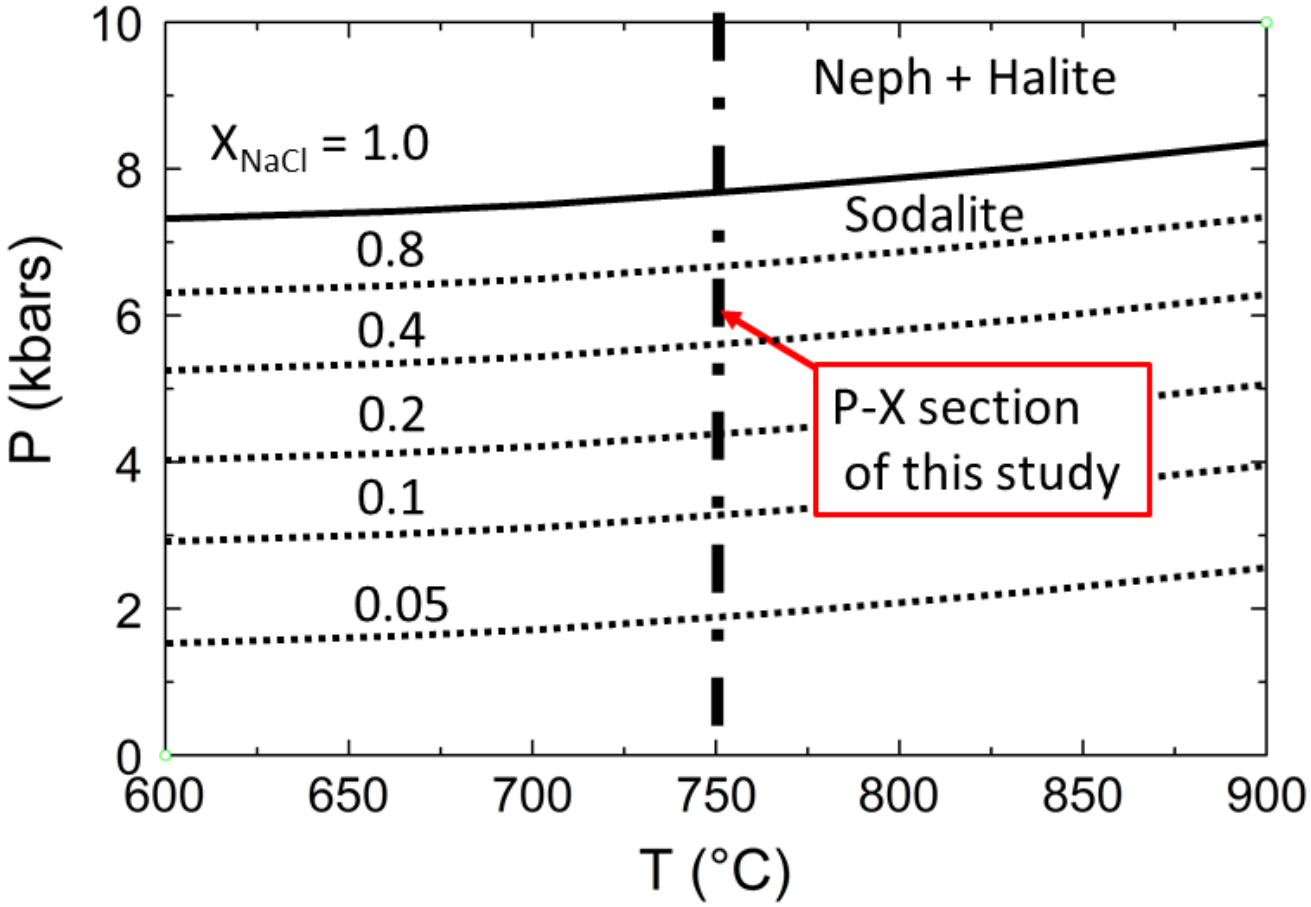
10
8
6
4
2
0
P (kbars)
600
650
700
750
800
850
900
T (°C)
Neph + Halite
X_{NaCl} = 1.0
Sodalite
0.8
0.4
0.2
0.1
0.05
P-X section
of this study

Figure 2

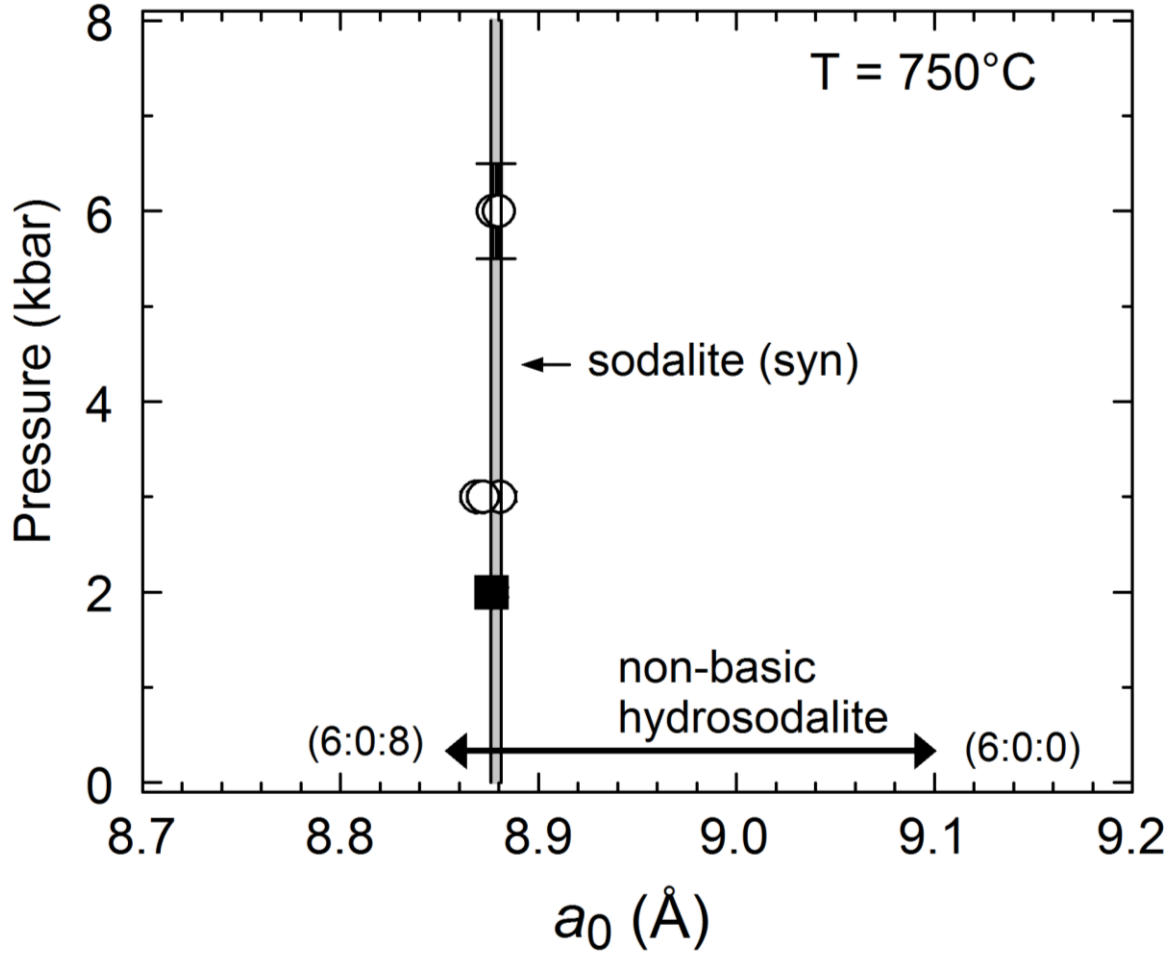
T = 750°C
Pressure (kbar)
sodalite (syn)
non-basic
hydrosodalite
(6:0:8)
(6:0:0)
a_0 (Å)
0
2
4
6
8
8.7
8.8
8.9
9.0
9.1
9.2

Figure 3

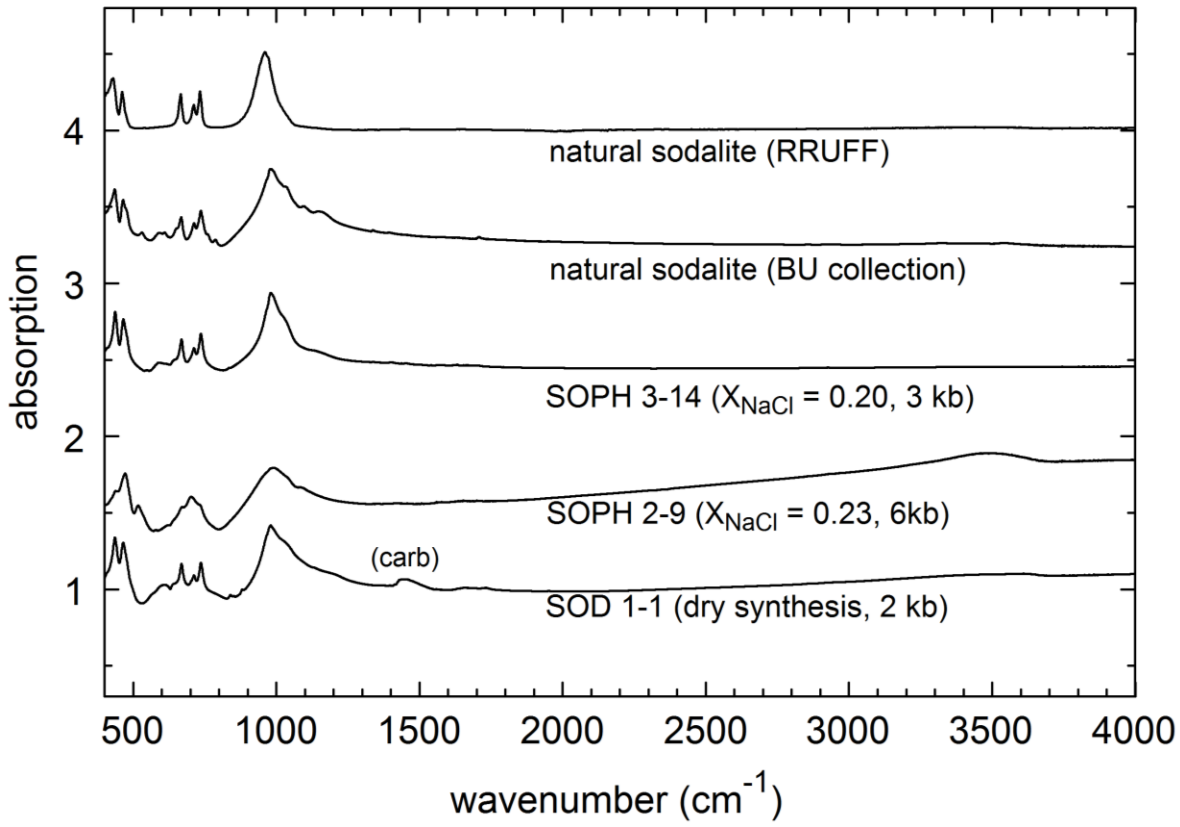
absorption
4
3
2
1
natural sodalite (RRUFF)
natural sodalite (BU collection)
SOPH 3-14 (X_{NaCl} = 0.20, 3 kb)
SOPH 2-9 (X_{NaCl} = 0.23, 6kb)
(carb)
SOD 1-1 (dry synthesis, 2 kb)
500
1000
1500
2000
2500
3000
3500
4000
wavenumber (cm^{-1})

Figure 4

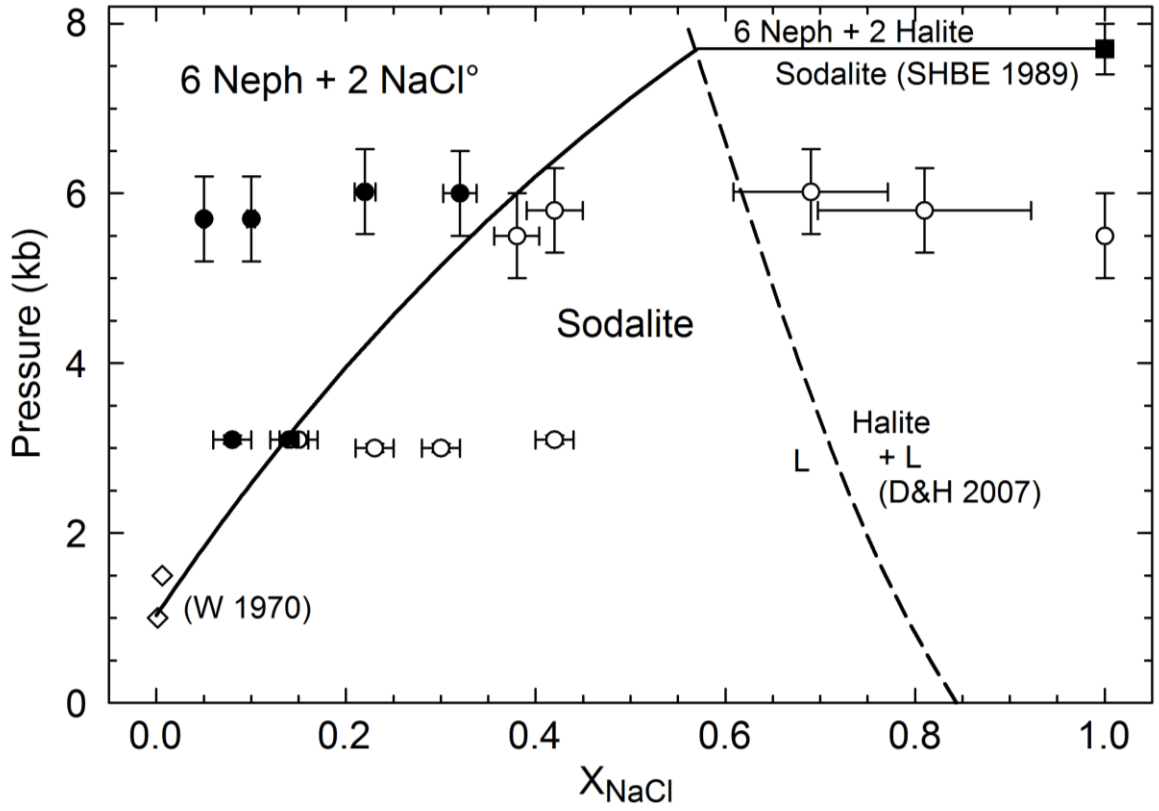
6 Neph + 2 NaCl°
6 Neph + 2 Halite
Sodalite (SHBE 1989)
Sodalite
Halite
+ L
(D&H 2007)
L
(W 1970)
Pressure (kb)
X_{NaCl}
0
2
4
6
8
0.0
0.2
0.4
0.6
0.8
1.0

Figure 5

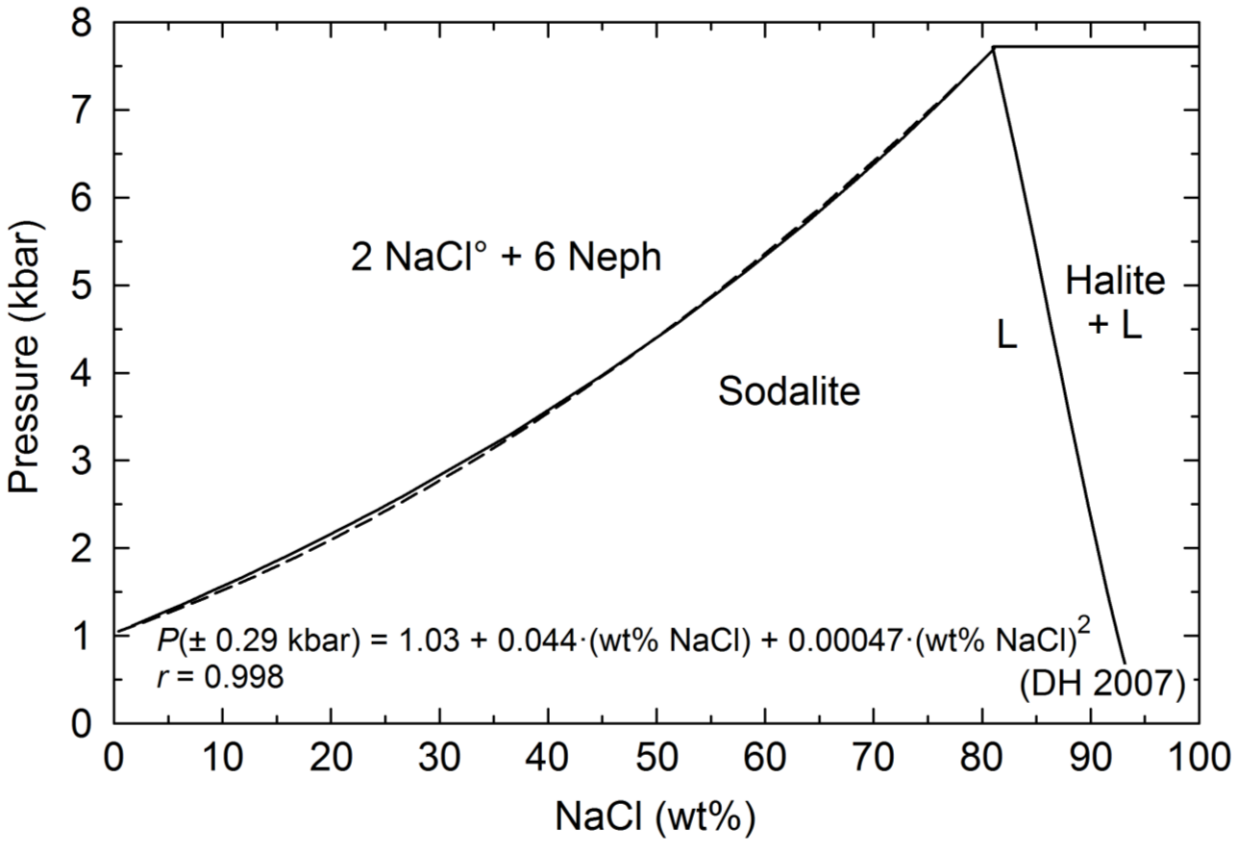
Pressure (kbar)
NaCl (wt%)
2 NaCl° + 6 Neph
Sodalite
L
Halite
+ L
P(± 0.29 kbar) = 1.03 + 0.044·(wt% NaCl) + 0.00047·(wt% NaCl)2
r = 0.998
(DH 2007)

Figure 6

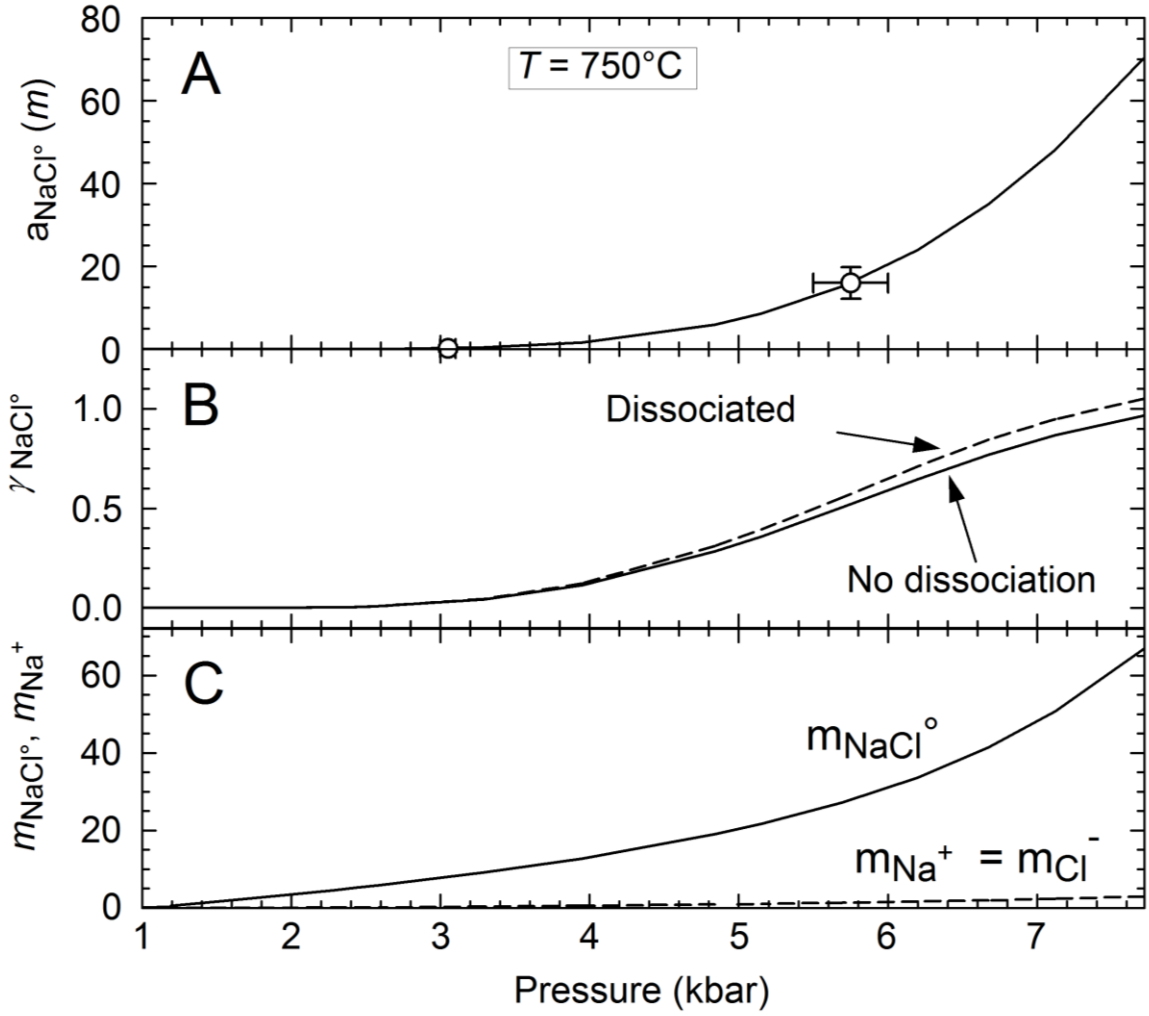
A
T = 750°C
a NaCl° (m)
B
Dissociated
No dissociation
γ NaCl°
C
m NaCl°
m Na+ = m Cl-
m NaCl°, m Na+
Pressure (kbar)

Figure 7.

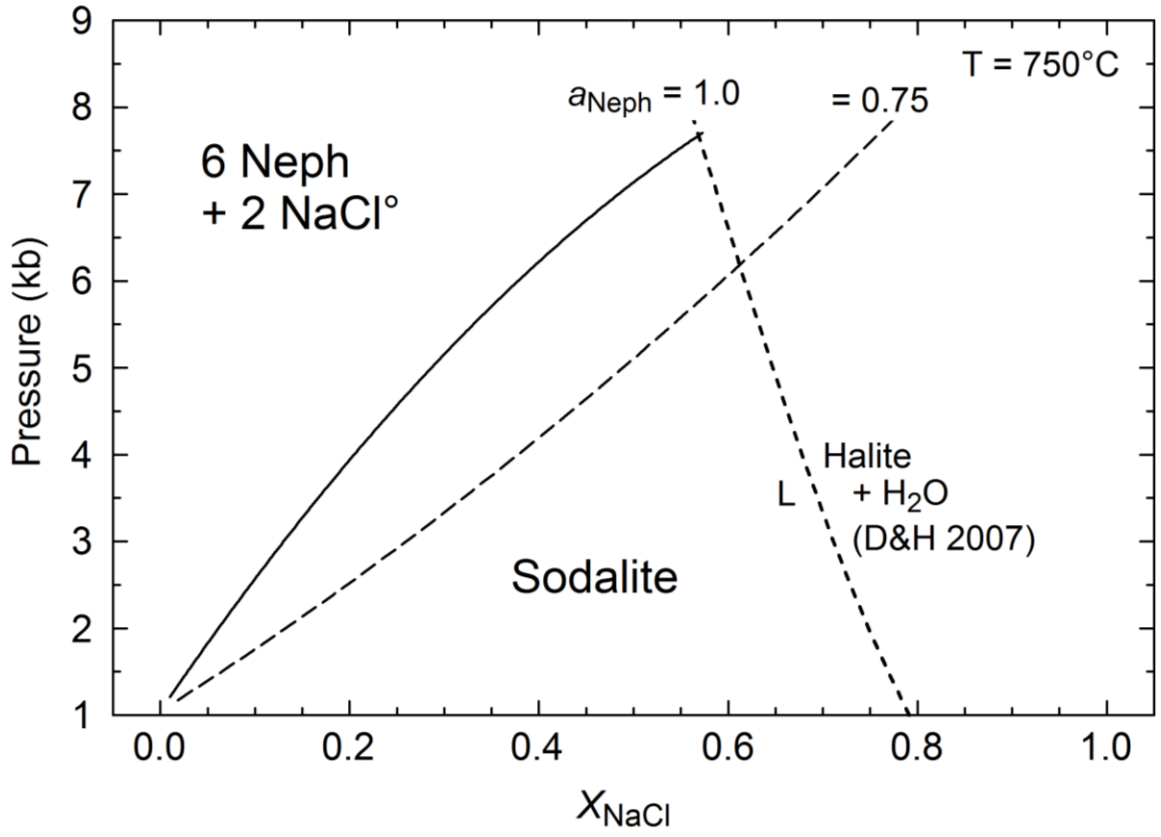
T = 750°C
a_{Neph} = 1.0
= 0.75
6 Neph
+ 2 NaCl°
Halite
+ H_2O
(D&H 2007)
L
Sodalite
Pressure (kb)
X_{NaCl}
9
8
7
6
5
4
3
2
1
0.0
0.2
0.4
0.6
0.8
1.0